Algal Research 78 (2024) 103390

Contents lists available at ScienceDirect

Algal Research

journal homepage: www.elsevier.com/locate/algal

Influence of biotic and abiotic factors on prymnesin profiles in three strains of *Prymnesium parvum*

Catherine C. Bannon [a,b], Xinhui Wang [c], Silvio Uhlig [d], Ingunn A. Samdal [d], Pearse McCarron [b], Thomas Ostenfeld Larsen [c], Elizabeth M. Mudge [b,*]

[a] *Department of Biology, Dalhousie University, Halifax, NS B3H 4R2, Canada*
[b] *Biotoxin Metrology, National Research Council Canada, 1411 Oxford Street, Halifax, NS B3H 3Z1, Canada*
[c] *Department of Biotechnology and Biomedicine, Technical University of Denmark, Søltofts Plads, Building 221, 2800 Kgs. Lyngby, Denmark*
[d] *Norwegian Veterinary Institute, P.O. Box 64, 1431 Ås, Norway*

ARTICLE INFO

Keywords:
Prymnesins
Ichthyotoxin
Harmful algal blooms
Prymnesium parvum
LC–HRMS
Golden alga
Haptophyte

ABSTRACT

Harmful algal blooms of *Prymnesium parvum* have resulted in significant fish kill events globally. These haptophytes produce the ichthyotoxic prymnesins, large polyethers categorized into A-, B- and C-types based on their carbon backbones with several analogs varying by the degree of glycosylation, chlorination, and double bonds. However, the influence of various biotic or abiotic factors on prymnesin profiles remains unknown. We investigated the influence of growth phase, nitrogen availability, light intensity, and salinity on prymnesin profiles of three *P. parvum* strains (UTEX-2797, K-0374 and PPSR01). Strains were selected based on their chemotypic expression of the three prymnesin backbones. Results demonstrated that different growth conditions led to strain-specific changes in prymnesin profiles. In the stationary phase, increased glycosylation was observed compared to the exponential growth phase for all strains. Additionally, at early stationary phase the trichlorinated analogs represented >90 % of all prymnesins of *P. parvum* strains UTEX-2797 and PPSR01 when cultured at salinity of 10 psu. By gaining an understanding of the effects of biotic and abiotic factors, culture conditions could be modified to promote specific prymnesin profiles to support the development of analytical reference materials. Furthermore, evaluating prymnesin profiles in combination with toxicity assays will provide insights into prymnesin biosynthesis, mode of action and toxicity.

1. Introduction

Prymnesium parvum is a haptophyte species, sometimes referred to as golden alga, responsible for fish-killing events leading to significant economic and ecological losses globally [1–3]. One of the most recent disastrous fish kills was observed in the Oder River in 2022 where a *P. parvum* bloom resulted in the death of over 200 t of fish [4,5]. Toxicity has been attributed to a class of allelopathic ichthyotoxins called prymnesins, which are large (1600–2300 Da) ladder-framed polyether compounds that are categorized into A-, B- and C-types based on number of carbons in their aglycone backbone (A-type: 91 carbons, B-type: 85 carbons, C-type: 83 carbons) [6–9]. To date, four prymnesins have been structurally elucidated (Fig. 1). Prymnesin-1 and prymnesin-2 are A-type prymnesins that were characterized by Igarashi, et al. [8,10]. The more recently characterized B-type prymnesins are prymnesin-B1 and prymnesin-B2 [9], which lack the H—I fused ether rings of the A-type and are replaced with a short three-carbon chain. The backbone structure of C-type prymnesins has not yet been elucidated [9]. Many additional analogs have been detected in *P. parvum* using LC–MS methods for each structural backbone, with variations in the number of double bonds, degree of oxidation, chlorination and glycosylation [11]. *P. parvum* strains are classified into three separate chemotypic lineages that are reported to only produce a single prymnesin type, although there is a considerable degree of variation in analogs in any given strain [11].

Various studies have investigated the influence of biotic and abiotic factors such as nutrient availability (nitrogen and phosphorus), pH, light and salinity on *P. parvum* growth and toxicity with a focus on conditions that support toxic blooms [7]. Similar to other harmful algae, differences in strain-specific toxicity and prymnesin cell quotas have been observed [1,12]. Prymnesin-1 (A-type), was six times more toxic than prymnesin-B1 using a fish gill cell line, suggesting that prymnesin backbones may

* Corresponding author at: National Research Council of Canada, 1411 Oxford Street, Halifax, NS, Canada.
E-mail address: elizabeth.mudge@nrc-cnrc.gc.ca (E.M. Mudge).

https://doi.org/10.1016/j.algal.2024.103390
Received 29 September 2023; Received in revised form 13 December 2023; Accepted 2 January 2024
Available online 6 January 2024

influence toxicity [9]. Various reports have indicated that the hemolytic activity of *P. parvum* increases during stationary phase compared to exponential growth phase [13–15] and nutrient limitation has consistently resulted in increased culture toxicity independent of growth rate [7,15–17]. Contradictory results have been observed when evaluating the influence of other abiotic factors, such as salinity, pH and light, suggesting strain-specific variations in response [18–21]. However, the majority of these investigations have relied on in vitro bioassays for toxicity determination where the profiles of specific prymnesin analogues nor prymnesin content was not directly evaluated.

A major limiting factor impeding prymnesin quantitation and profiling is the lack of available reference materials. A method for indirect quantitation of prymnesins uses fluorescence tagging of the primary amine to measure prymnesin cell quotas by HPLC–FLD, but does not distinguish between toxin backbones or individual analogs [22]. In order to advance prymnesin research, it is imperative to develop reference materials for these toxins, with various backbones and structural variants to enable comparative measurements for prymnesins across analytical methodologies, evaluate bioassay toxicity and pursue environmental monitoring.

The focus of this study was to investigate the biotic and abiotic factors that influence prymnesin profiles in three *P. parvum* strains (UTEX-2797, K-0374, PPSR01), selected based on their production of A-, B- and C-type prymnesins, respectively. Prymnesin profiles were evaluated at time points representing exponential, early stationary and late stationary growth phases. Nitrogen availability, salinity and light conditions were assessed to evaluate species-specific prymnesin expression in response to abiotic factors. The results provide new insights into factors that influence prymnesin production, which have importance in toxicity studies, analytical metrology, and environmental monitoring.

2. Material and methods

2.1. Reagents

Methanol (MeOH), acetonitrile (MeCN), and formic acid (~98 %) were LC–MS grade from Thermo Fisher Scientific (Ottawa, ON, Canada). Distilled water was ultra-purified to 18.2 MΩ × cm using a Milli-Q water purification system (Millipore Sigma, Oakville, ON, Canada). Artificial seawater was prepared with Instant Ocean® sea salt (Blacksburg, VA).

2.2. P. parvum cultures

Three non-axenic strains of *P. parvum* UTEX-2797, K-0374, and PPSR01, were used to investigate A-type, B-type and C-type prymnesin profiles, respectively. UTEX-2797 was isolated in 2001 from the Texas Colorado River, TX, USA, K-0374 was isolated in Norway in 1989 and PPSR01 was isolated from the Serpentine River, WA, Australia in 2000, as described previously [11].

2.3. Experimental setup

Prymnesin profiles were evaluated in *P. parvum* cultures at different growth stages and from the influence of several abiotic factors. Harvest dates were established based on an initial growth curve study in L1 (−Si)) media under controlled (growth phase) culture conditions. During the growth phase experiment (Section 2.3.1), the cultures were harvested on days 6, 14 and 30 representing exponential, early stationary and late stationary phases, respectively. For experiments investigating the influence of abiotic factors (Sections 2.3.2–2.3.4), samples were collected on days 10 and 30. Prior to use, cultures were acclimated in the treatment medium for a minimum of two weeks prior to each study.

2.3.1. Growth phase (control conditions)

The PPSR01 and K-0374 cultures were grown in biological triplicates ($n = 3$) and duplicates for *P. parvum* UTEX-2797 ($n = 2$). Cultures were inoculated at 1:20 dilution into 100 mL of filter (0.22 μm) sterilized L1 (−Si)) media prepared to pH 8.2 [23], 24N:1P (0.88 mM N and 0.036 mM P) and 30 psu with Instant Ocean sea salt. Experimental cultures were grown at 20 °C under 30 μmol m^{-2} s^{-1} cool white light with a 12:12 light cycle.

2.3.2. Nitrogen

Filter-sterilized L1(−Si)) medium was prepared with Instant Ocean (30 psu) and L1 trace metal mix to 10N:1P ratio (0.39 mM N and 0.036 mM P), a low nitrogen to phosphorus ratio used in literature to investigate the influence of nutrients on *P. parvum* growth [24]. The

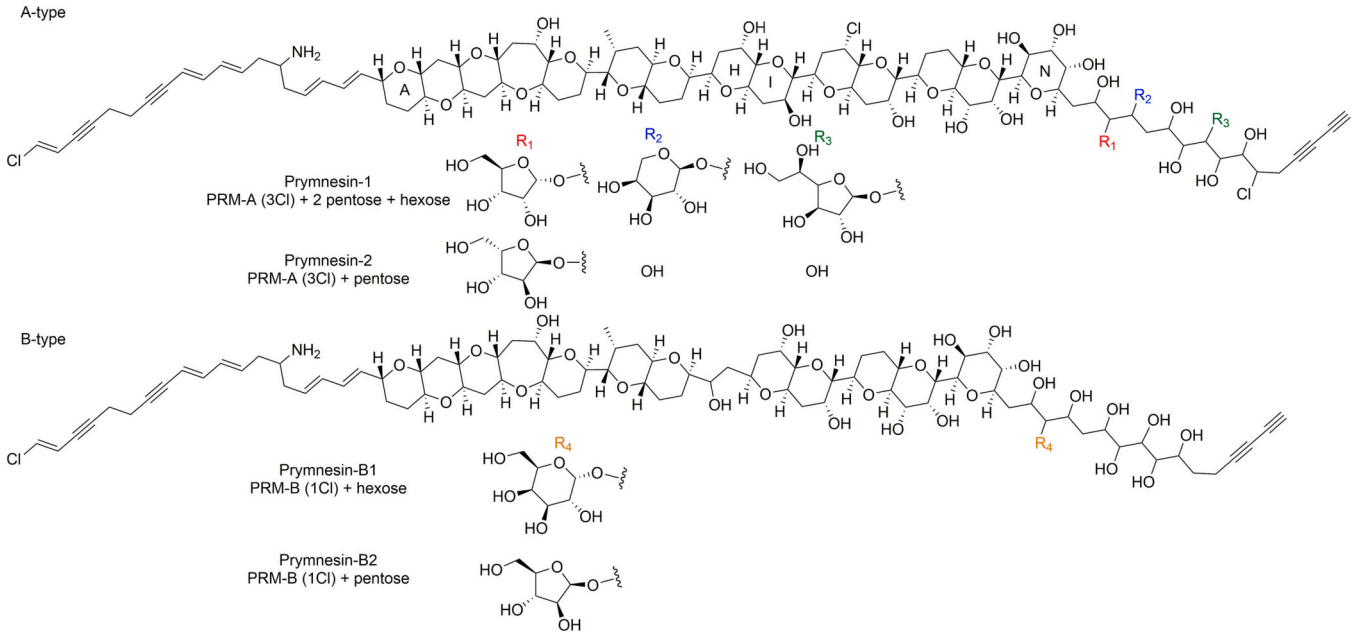

Fig. 1. Structures of characterized A-type prymnesins (prymnesin-1 and prymnesin-2), and B-type prymnesins (prymnesin-B1 and prymnesin-B2) produced by *Prymnesium parvum*.

acclimated 10N:1P culture of each strain was inoculated at a 1:20 dilution, in duplicate, with 75 mL of either 24N:1P, the standard ratio of L1(−Si)) media, or 10N:1P media. Cultures were then grown at 20 °C, under 30 μmol m^{-2} s^{-1} irradiance with a 12:12 light cycle.

2.3.3. Salinity

L1(−Si)) medium was prepared with Instant Ocean to 10 psu and 30 psu salinity and both were filter-sterilized. Salinity was measured using a refractometer (AGATO S-10). The 10 psu cultures of each strain were inoculated at a 1:20 dilution, in duplicate, with 75 mL of either 10 psu and 30 psu media. All cultures were then grown at 20 °C, under 30 μmol m^{-2} s^{-1} irradiance with a 12:12 light cycle.

2.3.4. Light

Cultures were grown in filter-sterilized L1(−Si)) media prepared to 30 psu salinity as described in Section 2.3.1. The high light conditions were determined to be 100 μmol m^{-2} s^{-1} irradiance, measured using a light reader (LI-COR, LI-250A). Acclimated high-light cultures were inoculated in a 1:20 dilution into 75 mL of L1(−Si)) medium. Cultures for each strain ($n = 2$) were either grown under 100 μmol m^{-2} s^{-1} irradiance or 30 μmol m^{-2} s^{-1} irradiance. Both incubators were maintained at 20 °C with a 12:12 light cycle. Due to an incubator malfunction, the high-light cultures were lost before the final harvest at day 30.

2.3.5. Cell counts and growth rate calculations

Cell counts were taken every second day throughout each experimental set-up. For this, 300 μL of each biological replicate was combined with 2 μL of acidified Lugol's iodine reagent. Duplicate cell counts were taken using 10 μL of vortex-mixed samples on a Countess FL II cell counter (Invitrogen, Thermo Fisher).

Growth rates (d^{-1}) were calculated using the linear regression of natural logarithm cell counts over time during exponential phase of growth. Two-tailed *t*-tests were performed to determine the significance ($p < 0.05$) of treatments on growth rates.

2.4. P. parvum harvesting

Aliquots (10 mL) from each experimental condition, growth phase and biological replicate were harvested by centrifugation (3440 ×*g* for 20 min) to obtain cellular pellets. The supernatants were transferred to clean scintillation vials. Both the cell pellets and supernatant from all samples were stored at −20 °C until extraction.

2.4.1. Cellular pellet extraction

Cell pellets were extracted with MeOH (10 mL) and vortex-mixed until homogenous. The extracts were sonicated on ice (2 min; 2 s on, 3 s off; 40 % amplitude) using a probe sonicator (Qsonica, C.T., USA, Model Q500), followed by centrifugation (3440 ×*g* for 10 min). The MeOH was decanted into clean vials and evaporated to dryness using a vacuum concentrator at 45 °C (Savant SPD2010, SpeedVac Concentrator). The residues were dissolved in MeOH (500 μL) and filtered (0.45 μm PVDF centrifugal filters; Millipore Sigma) prior to analysis.

2.4.2. Media extraction

One replicate from each treatment was extracted to determine whether prymnesins were released into the media. 500 mg C18 Supelco SPE cartridges (Millipore Sigma) were pre-conditioned with MeOH (3 mL) followed by H_2O (3 mL). The supernatant (10 mL) was slowly loaded onto the cartridge before washing with H_2O (3 mL). The cartridges were eluted with MeOH (3 mL) and evaporated to dryness under N_2 gas (35 °C). Residues were dissolved in MeOH (100 μL) and filtered through 0.45 μm PVDF centrifugal filters prior to analysis.

2.5. LC-MS Analysis

2.5.1. Untargeted prymnesin profiling by LC–HRMS

An Agilent 1290 Infinity II LC equipped with a binary pump, temperature-controlled autosampler (10 °C) and column compartment (40 °C) (Agilent Technologies, Mississauga, ON, Canada) coupled to a Q Exactive HF Orbitrap mass spectrometer (ThermoFischer Scientific) with a heated electrospray ionization probe (HESI-II). Chromatographic separation was achieved using a Hypersil GOLD C18 column (ThermoFisher Scientific, 100 × 2.1 mm, 1.9 μm) using a different gradient for each prymnesin type with mobile phases composed of 0.1 % formic acid in both H_2O (A) and MeCN (B). The flow rate and injection volumes were 0.4 mL min^{-1} and 5 μL, respectively. The 'A-type' gradient used for *P. parvum* UTEX-2797 samples was: 0–10 min, 42–50 % B; 10–10.1 min, 50–99 % B; 10.1–12 min, 99 % B; followed by a 3 min re-equilibration at 42 % B. The 'B-type' gradient used for *P. parvum* K-0374 samples was: 0–10 min, 40–49 % B; 10–10.1 min, 49–99 % B; 10.1–12 min, 99 % B; followed by a 3 min re-equilibration at 40 % B. The 'C-type' gradient used for *P. parvum* PPSR01 samples was: 0–10 min, 34–44 % B; 10–10.1 min, 44–99 % B; 10.1–12 min, 99 % B; followed by a 3 min re-equilibration at 34 % B.

Full-scan acquisition was performed from *m/z* 800–2300 in positive mode. The spray voltage of the source was +4.5 kV, with a capillary temperature of 340 °C. The sheath and auxiliary gas were set at 40 and 10 (arbitrary units). The auxiliary gas heater temperature was set at 150 °C and the S-Lens RF level was set to 100. The mass resolution setting was 240,000 with an automatic gain control (AGC) target of 5×10^6 and a maximum injection time of 512 ms per scan.

2.5.2. Targeted Prymnesin Profiling by LC–MS/MS

An Agilent 1260 LC equipped with a binary pump, temperature-controlled autosampler (10 °C) and temperature-controlled column compartment (40 °C) was coupled to a 4000 QTRAP mass spectrometer (Sciex, Concord, ON, Canada) with a turbospray ionization source. Selected reaction monitoring (SRM) acquisition was performed with positive ionization of the doubly charged prymnesin ions using a unique transition list for each prymnesin based on the most dominant analogues detected in the untargeted LC–HRMS acquisition (Table 1) based on prymnesins identified by Binzer et al. (2019). The spray voltage of the source was +5.0 kV, with a capillary temperature of 300 °C, and a declustering potential of 70. Chromatographic separation was the same as that used in Section 2.5.1.

2.5.3. Data Analysis

Prymnesin profiles were determined by measuring the peak area of the most abundant transition for each prymnesin analogue in the SRM transitions list (Table 1). The peak area was adjusted to peak area per cell to estimate the prymnesin cell quotas, however no quantitative data is available at this time due to the lack of available reference materials. Prymnesin profiles were adjusted to a relative scale based on proportions of the prymnesin analogues in each experimental condition to determine relative changes in profiles based on response to biotic and abiotic factors.

3. Results

3.1. Strain-specific growth curves and LC–HRMS screening of prymnesin analogs

Three *P. parvum* strains, each belonging to a different chemotype, were selected to investigate the influence of growth phase, light, salinity and nitrogen availability on prymnesin production. Cell counts were taken every second day until early stationary phase to determine the appropriate harvesting dates and monitor the influence conditions had on growth rate. Growth curves of each strain acquired during the growth phase study are presented in Fig. 2. The growth curves from the other

Table 1
LC-HRMS and LC–MS/MS details for the dominant prymnesins detected in the three *P. parvum* strains.

P. parvum strain	Prymnesin analog	Neutral formula	Accurate mass (*m/z*; $[M + 2H]^{2+}$	Mass error (ppm)	Retention time (min; LC–HRMS)	SRM transition (*m/z* precursor→*m/z* product)	CE (eV)
UTEX-2797 A-type	PRM-A (3 Cl) + pentose (prymnesin-2)	$C_{96}H_{136}Cl_3NO_{35}$	984.9068	1.6	5.75	986 → 920	20
	PRM-A (2 Cl) + pentose	$C_{96}H_{137}Cl_2NO_{35}$	967.9251	0.4	5.33	969 → 903	20
	PRM-A (3 Cl) + 2 pentose + hexose (prymnesin-1)	$C_{107}H_{154}Cl_3NO_{44}$	1131.9531	0.3	4.73	1133 → 920	30
	PRM-A (2 Cl) + 2 pentose + hexose	$C_{107}H_{155}Cl_2NO_{44}$	1114.9725	0.2	4.46	1116 → 903	30
K-0374 B-type	PRM-B (2 Cl) + pentose	$C_{90}H_{129}Cl_2NO_{33}$	911.8983	−0.2	5.33	913 → 847	20
	PRM-B (1 Cl)	$C_{85}H_{122}ClNO_{29}$	828.8975	0.8	4.97	830 → 812	20
	PRM-B (1 Cl) + pentose (prymnesin-B2)	$C_{90}H_{130}ClNO_{33}$	894.9161	−2.1	4.87	896 → 830	20
	PRM-B (1 Cl) + pentose + hexose	$C_{96}H_{140}ClNO_{38}$	975.9442	−0.2	4.16	977 → 830	20
PPSR01 C-type	PRM-C (3 Cl) + pentose	$C_{88}H_{126}Cl_3NO_{35}$	931.8674	1.4	4.93	933 → 867	20
	PRM-C (3 Cl + DB) + pentose	$C_{88}H_{124}Cl_3NO_{35}$	930.8594	1.2	4.52	933 → 867	20
	PRM-C (2 Cl) + pentose	$C_{88}H_{127}Cl_2NO_{35}$	914.8860	0.5	4.47	915 → 849	20
	PRM-C (2 Cl + DB) + pentose	$C_{88}H_{125}Cl_2NO_{35}$	913.8779	0.2	4.08	915 → 849	20
	PRM-C (2 Cl + DB) + 2 pentose + hexose	$C_{99}H_{143}Cl_2NO_{44}$	1060.9281	2.6	3.33	1062 → 849	20
	PRM-C (2 Cl) + 2 pentose + hexose	$C_{99}H_{145}Cl_2NO_{44}$	1061.9354	2.2	3.66	1062 → 849	20
	PRM-C (3 Cl) + 2 pentose + hexose	$C_{99}H_{144}Cl_3NO_{44}$	1078.9165	2.7	3.98	1080 → 867	20
	PRM-C (3 Cl + DB) + 2 pentose + hexose	$C_{99}H_{142}Cl_3NO_{44}$	1077.9090	3.0	3.62	1080 → 867	20

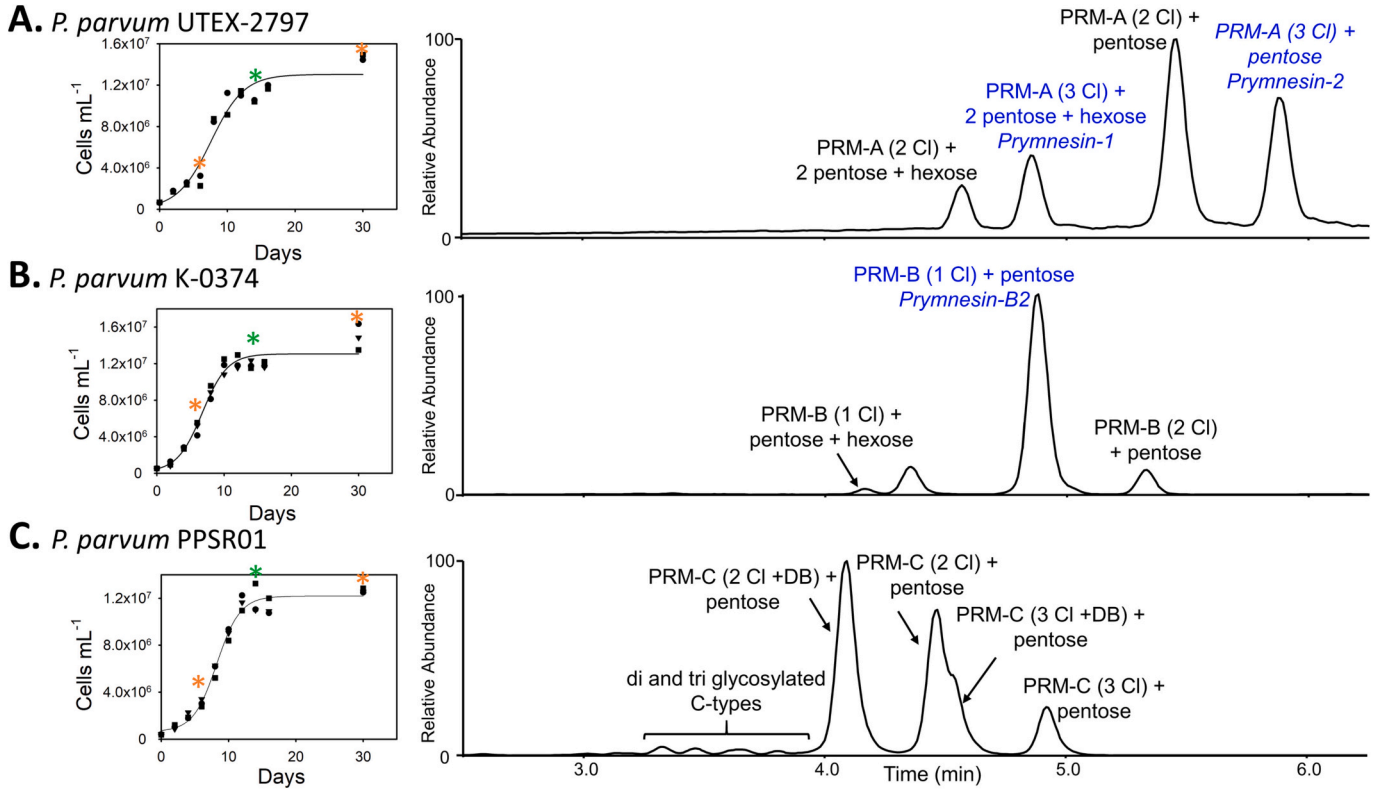

Fig. 2. Growth curves and corresponding LC–HRMS total ion chromatograms (*m/z* 800–2300) for (A) *P. parvum* UTEX-2797, (B) *P. parvum* K-0374 and (C) *P. parvum* PPSR01. The harvest dates for the growth phase experiment are indicated by (*) symbols. Solid symbols (▼, ●, ■) represent biological replicates. The green star indicates the sample (day 14) associated with the representative LC–HRMS total ion chromatogram. The structurally characterized prymnesins are labelled in blue, and the other dominant prymnesin analogs detected across the experimental studies are labelled in black. (For interpretation of the references to colour in this figure legend, the reader is referred to the web version of this article.)

treatments are presented in Fig. S1. During the growth phase experiment, the growth rates of *P. parvum* K-0374 ($r = 0.37 \pm 0.01$) was higher than for *P. parvum* UTEX-2797 ($r = 0.29 \pm 0.02$) and *P. parvum* PPSR01 ($r = 0.30 \pm 0.01$) (Table 2). For all strains grown during this trial, exponential phase occurred from day 2 to day 8, followed by stationary phase (when $r = 0$) beginning around day 10. The samples harvested on day 6 were representative of exponential phase, while those on days 14 and 30 were of early- and late-stationary phases, respectively.

Table 2
Experimental treatment details and significance data of *P. parvum* growth rates ($r \pm$ SD) of three *P. parvum* strains used to investigate the influence of biotic and abiotic factors on prymnesin profiles.

Experiment	Biological replicates	Harvest (day)	Treatment	UTEX2797 A-Type	K0374 B-type	PPSR01 C-type
				Growth rate (day^{-1}) $r \pm$ SD		
Growth phase[b]	3[a]	6	Exponential	0.29 ± 0.02	0.37 ± 0.01	0.30 ± 0.01
		14	Early stationary			
		30	Late stationary			
Nitrogen	2	10, 30	24N:1P	0.30 ± 0.01	0.35 ± 0.01	0.27 ± 0.02
			10N:1P	0.32 ± 0.01	0.36 ± 0.00	0.25 ± 0.01
			p-value (24N:1P vs 10N:1P)	0.279	0.577	0.594
Salinity	2		30 psu	0.34 ± 0.02	0.36 ± 0.02	0.33 ± 0.02
			10 psu	0.25 ± 0.00	0.37 ± 0.03	0.21 ± 0.02
			p-value (30 psu vs 10 psu)	0.063	0.800	0.051
Light	2		30 μmol m^{-2} s^{-1}	0.40 ± 0.01	0.46 ± 0.02	0.33 ± 0.02
			100 μmol m^{-2} s^{-1}	0.40 ± 0.03	0.37 ± 0.02	0.25 ± 0.00
			p-value (30 μmol m^{-2} s^{-1} vs 100 μmol m^{-2} s^{-1})	0.924	0.107	0.073

p-values determined using two-tailed t-test (significance at 95 % confidence, n = 2 for each treatment).
[a] UTEX 2797, n = 2 (broken flask).
[b] Conditions: 24N:1P, 30 psu, 30 μmol m^{-2} s^{-1} and 20 °C.

Cell counts were monitored during the abiotic treatment studies to evaluate the influence of the different conditions on growth rates. There were no statistically significant differences between any growth rates for all strains when comparing each condition (*p*-values >0.05), however there were only duplicates in each treatment minimizing statistical power (Table 2). When comparing the nitrogen treatments, all cultures grown under low N:P conditions (10N:1P) reached stationary phase faster resulting in a decreased population size compared to cultures grown under nitrogen replete conditions (24N:1P) (Fig. S1). *P. parvum* K-0374 and PPSR01 showed decreases in maximum population size when grown in 10 psu salinity compared to 30 psu (Fig. S1). Samples of each replicate were harvested on day 10 and day 30 (Fig. S1). The growth phase of samples harvested on day 10 differed depending on conditions (i.e. 10N:1P was in stationary phase), however all samples were in late stationary phase by day 30.

Representative LC–HRMS full-scan chromatograms of each strain in early stationary phase are presented (Fig. 2) where each strain produced one prymnesin type, with multiple analogs, as described by Binzer, et al. [11]. The four dominant prymnesin analogs detected in *P. parvum* UTEX-2797 were prymnesin-1, prymnesin-2, PRM-A (2 Cl) + pentose and PRM-A (2 Cl) + 2 pentose + hexose (Fig. 2D). In *P. parvum* K-0374, prymnesin-B2, PRM-B (2 Cl) + pentose and PRM-B (1Cl) + pentose + hexose were most abundant (Fig. 2E). Notably, no prymnesin-B1, one of the two structurally characterized B-Type prymnesins, was detected in this culture. *P. parvum* PPSR01 was more complex with numerous double-bond-containing backbones and increased levels of glycosylation [11]. The four dominant peaks were PRM-C (2 Cl + DB) + pentose, PRM-C (2 Cl) + pentose, PRM-C (3 Cl + DB) + pentose and PRM-C (3 Cl) + pentose (Fig. 2F). PRM-C (2 Cl) + pentose and PRM-C (3 Cl + DB) + pentose co-eluted; however, distinct peaks were measured due to variations in their SRM transitions (Fig. S2). Additionally, di- and tri-glycosylated prymnesin analogs eluted from 3.6 to 4.0 min, revealing the presence of a complex mixture of unidentified prymnesins. Of these analogs, the most dominant were included in the SRM transition list (Table 1).

The LC–HRMS identification of the dominant prymnesin analogs in the cultures informed the SRM transitions selected for targeted LC–MS/MS method development (Fig. S2). The LC–MS/MS acquisition provided semi-quantitative data for measuring prymnesin analogs, but given the lack of analytical reference materials, absolute quantitation of prymnesin analogs was not feasible. Prymnesin cell quotas were estimated by combining the peak areas (of the molecular ion transition) for each prymnesin and adjusting for cell concentration (total prymnesin per cell). However, this assumes that all prymnesin analogs of have a similar MS response. Due to these limitations, comparisons will only be made between each treatment condition (control vs. treatment) within a species, with observations of general trends in prymnesin cell quotas between conditions and strains.

The prymnesin profiles described focus on the intracellular prymnesins in the cellular pellets. Samples of the media were analyzed to determine the level of extracellular prymnesins. In *P. parvum* UTEX-2797, <3 % of total prymnesin peak-area-per-cell was present in the media across all treatments (Fig. S3). In *P. parvum* K-0374, the percent of total prymnesin peak area present in media was <3 % with the exception of 30 psucondition which had ~6 % of total prymnesins present in the medium (Fig. S3). Finally, <0.3 % of total prymnesin produced by *P. parvum* PPSR01 were present in the media (Fig. S3). Due to the low levels of prymnesins detected, the prymnesins profiles from the media were not included in the comparisons of the culture treatments.

3.2. Growth phase influence on prymnesin profiles

Four A-type prymnesins were monitored in *P. parvum* UTEX-2797 to investigate changes in profiles during the growth phase study. Prymnesin-2 was dominant during exponential phase (day 6) (74 ± 3 %), however it only represented 29 ± 2 % per cell after 14 days and 26 ± 1 % after 30 days (Fig. 3A). Compared to exponential phase, there was a higher proportion of tri-glycosylated prymnesins and PRM-A (2 Cl) + pentose in later growth phases, which had similar prymnesin profiles at days 14 and 30. However, there was an increase in prymnesin cell quota in late stationary phase (Fig. S4).

Prymnesin-B2 dominated the profile of *P. parvum* K-0374 during the growth phase study (68–83 %). An increase in the proportion of PRM-B (1 Cl) + pentose + hexose and a relative decrease of PRM-B (2 Cl) + pentose was observed from exponential to stationary phase (Fig. 3B).

P. parvum PPSR01 produced a variety of prymnesin analogues with various levels of glycosylation, chlorination, and presence of double bonds in the backbones, consistent with data presented by Binzer et al. (2019). Eight dominant peaks were monitored across the treatments although additional analogs were observed at low abundances using LC–HRMS (Fig. 2, Table 1). In the growth phase experiments the prymnesin profiles changed substantially where during exponential phase, PRM-C (2 Cl + DB) + pentose and PRM-C (3 Cl + DB) + pentose dominated the profile (Fig. 3C). In early stationary phase, the proportion of the PRM-C (2 Cl) + pentose analog increased, while the profile remained primarily composed of pentose analogs. In late stationary phase there was a proportional increase of tri-glycosylated analogs relative to the earlier growth phases, including PRM-C (3Cl + DB) + 2

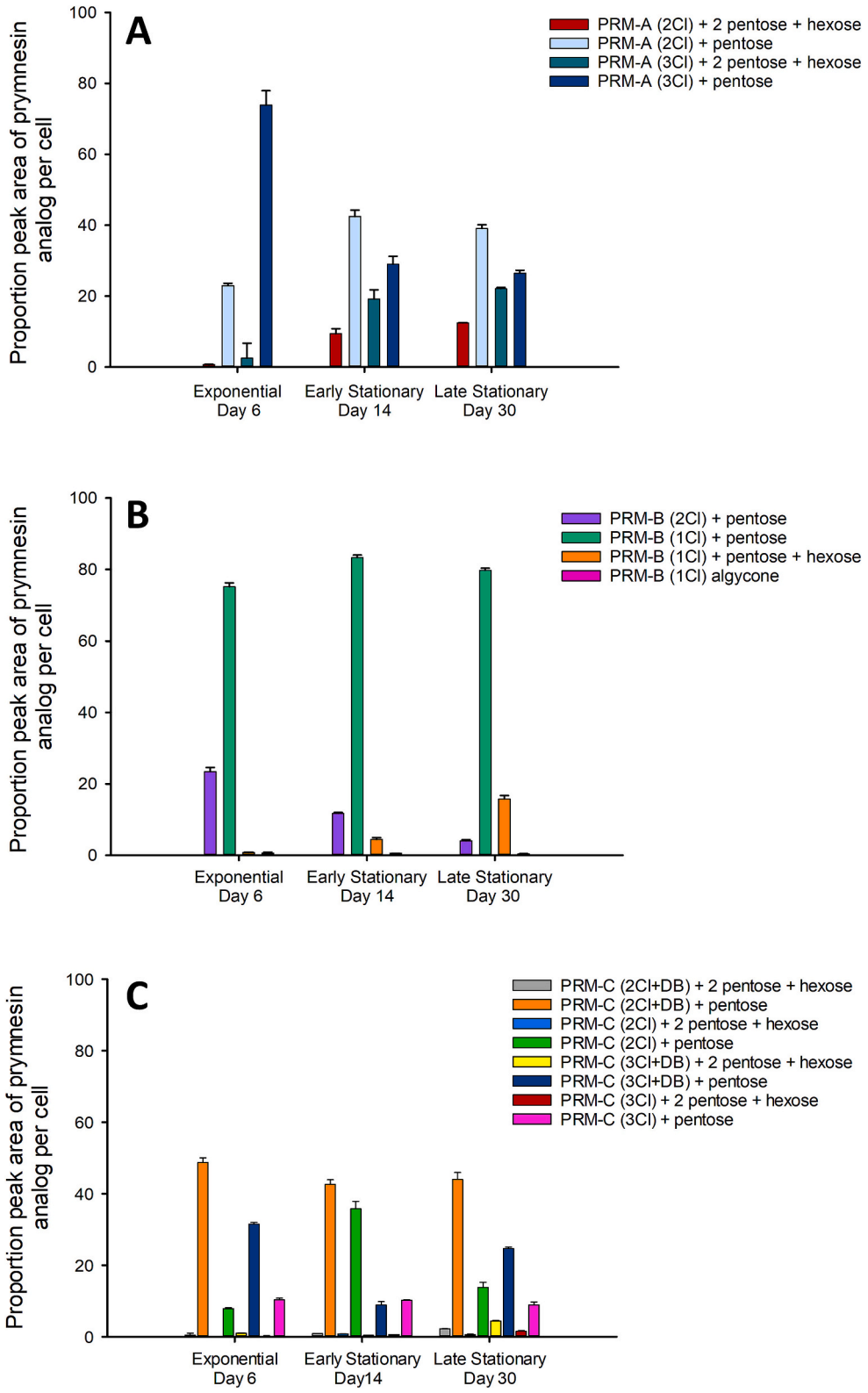

Fig. 3. Relative proportions of dominant prymnesin analogs in *P. parvum* UTEX-2797 (A), K-0374 (B) and PPSR01 (C) at different growth phases (exponential – day 6, early stationary – day 14, late stationary – day 30) (error bars = SD, $n = 2$ for A, $n = 3$ for B—C). Known prymnesins were (A) prymnesin-1: PRM-A (3Cl) + 2 pentose + hexose (dark green), prymnesin-2: PRM-A (3Cl) + pentose (dark blue) and (B) prymnesin-B2: PRM-B (1Cl) + pentose (teal). (For interpretation of the references to colour in this figure legend, the reader is referred to the web version of this article.)

pentose + hexose and PRM-C (2 Cl + DB) + 2 pentose + hexose.

3.3. Abiotic factors influencing A-type prymnesin profiles of P. parvum UTEX-2797

Abiotic factors were assessed in *P. parvum* UTEX-2797 cultures subsampled after 10 days. Low N:P conditions resulted in an increased proportion of prymnesin-1 and PRM-A (2 Cl) + 2 pentose + hexose compared to cells in high nitrogen conditions (24N:1P) (Fig. 4A). The highest proportion of prymnesin-1 (34 ± 1 %) was observed in low N:P media compared to all other treatments studied and cells had higher prymnesin cell quotas than those grown in high nitrogen media (Fig. S4). Growth at a low salinity (10 psu) led to higher proportions of prymnesin-2 than those grown at high salinity (30 psu) (Fig. 4B). Less than 5 % of prymnesin analogs in cells grown at low salinity had di-chlorinated backbones (Fig. S5). A greater proportion of prymnesin-1 was detected in cultures grown at higher light conditions (100 μmol m^{-2} s^{-1}) compared to low light (30 μmol m^{-2} s^{-1}) (Fig. 4C), which comprised 23.6 ± 0.1 % of the profiles at higher light compared to <6 % of those grown at the lower light. Total prymnesin cell quotas were higher in cells grown under high light to those grown at low light (Fig. S4).

After 30 days, the prymnesin profiles of cultures grown under various conditions were similar, with the exception of those grown at low salinity (Fig. 5). These conditions resulted in a higher proportion of tri-chlorinated prymnesins than all other treatments (Fig. S5). All conditions resulted in an increase in di-chlorinated prymnesins after 30 days compared to day 10 (Fig. S5). Similar trends occurred for the level of glycosylation, where the proportion of tri-glycosylated prymnesins increased after 30 days of growth with the exception of cultures grown in low N:P conditions (Fig. S5). These cultures had already reached stationary phase at day 10 (Fig. S1), which may have led to faster formation of tri-glycosylated prymnesins. Prymnesin cell quotas in *P. parvum* UTEX-2797 were approximately ten times higher in late stationary (day 30) phase than in exponential phase (day 6) (Fig. S4), while prymnesin cell quotas were variable across other treatments in late stationary phase (Fig. S4). The lowest total prymnesins were seen in cells grown at low N:P, and cultures grown at low salinity had lower prymnesin cell quotas than those grown at high salinity (Fig. S4).

3.4. Abiotic factors influencing B-type prymnesin profiles of P. parvum K-0374

After 10 days of growth, the B-type prymnesin profiles in *P. parvum* K-0374 showed minimal variability between the different nitrogen (Fig. 6A), salinity (Fig. 6B) and light (Fig. 6C) conditions. Prymnesin-B2 was the most dominant prymnesin under all conditions. A slightly higher proportion of the di-glycoside PRM-B (1 Cl) + pentose + hexose was produced in low N:P medium compared to high nitrogen medium, and in low salinity than in high salinity media. A small proportion of the aglycone PRM-B (1 Cl) was also detected after growth in 10 psu salinity. Prymnesin cell quotas were higher in the cultures grown at low light than at high light conditions and in low N:P medium than in higher nitrogen medium (Fig. S6).

After 30 days of growth, the *P. parvum* K-0374 cultures had similar prymnesin profiles regardless of growth conditions. Prymnesin-B2 was the most abundant analog, followed by PRM-B (1 Cl) + pentose + hexose and PRM-B (2 Cl) + pentose (Fig. 7). *P. parvum* K-0374 cells had increased levels of glycosylation and decreased levels of chlorination in stationary phase (Fig. S7). Compared to day 10 cultures, an increase in the PRM-B (1Cl) aglycone remained in the low salinity media, at approximately 3 % of the total prymnesin profile. This was the only exogenous aglycone analog detected across all strains and treatments. Within-treatment comparisons of the prymnesin cell quotas at day 30 showed the same general trends as those observed in *P. parvum* UTEX-2797 (Fig. S6B). Increased toxin levels were measured at late stationary phase compared to early stationary phase, in 24N:1P than in 10N:1P and in 30 psu salinity than in 10 psu.

3.5. Abiotic factors influencing C-type prymnesin profiles of P. parvum PPSR01

While eight C-type prymnesins were monitored and used to calculate prymnesin profiles, only the four dominant C-type prymnesins (pentose analogues) in *P. parvum* PPSR01 are presented in Fig. 8 to show the largest differences in the profiles. Detailed profiles of all eight analogs using stacked columns are summarized in Figs. S8–9. Considerable differences in C-type profiles were observed between abiotic conditions (Fig. 8A–C). A proportional increase of PRM-C (2 Cl) + pentose and PRM-C (3 Cl) + pentose compared to the analogs containing suspected double bonds was detected in cultures grown in 10N:1P media compared to 24N:1P media (Fig. 8A). Growth at 30 psu salinity was similar to other control samples, with PRM-C (2 Cl + DB) + pentose and PRM-C (3 Cl + DB) + pentose dominating the profile (Fig. 8C), while the profiles of cultures grown in 10 psu were dominated by PRM-C (3 Cl) + pentose and PRM-C (3Cl + DB) + pentose. Under low salinity, tri-chlorinated prymnesin analogs comprised over 90 % of total prymnesins (Fig. S10), while the prymnesin cell quotas under both salinity conditions were similar (Fig. S11). Cultures grown under high light conditions had an increased proportion of PRM-C (3 Cl) + pentose and higher prymnesin cell quotas than at low light conditions.

After 30 days of growth, there was an increase in the proportion of tri-glycosylated prymnesin analogs (Fig. S9; Fig. S10), with increased proportions of both PRM-C (3 Cl) + 2 pentose + hexose and PRM-C (3 Cl + DB) + 2 pentose + hexose across all treatments. The cultures harvested from the low salinity medium had an increased proportion of di-chlorinated analogs on day 30 compared to day 10, but the tri-chlorinated analogs remained dominant compared to the other

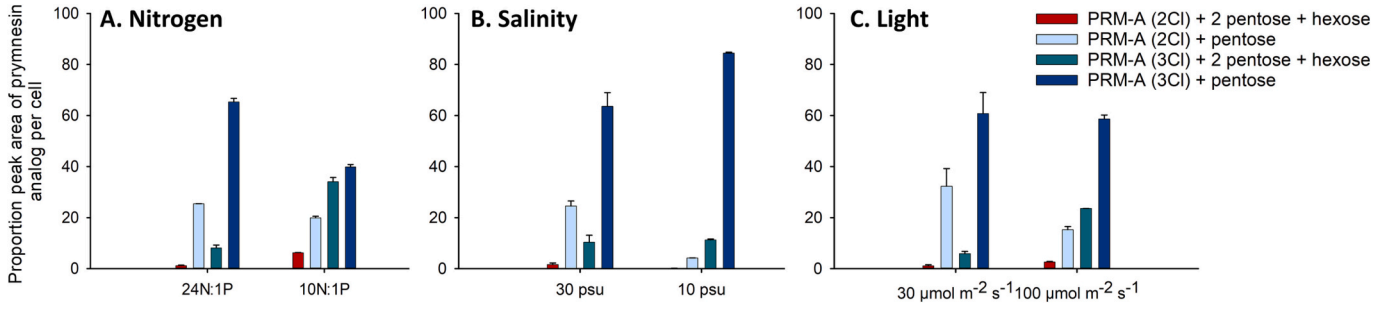

Fig. 4. Relative proportions of dominant A-type prymnesin analogs in *P. parvum* UTEX-2797 harvested at day 10 grown in different conditions: (A) nitrogen availability (24N:1P, 10N:1P) (B) salinity (30 psu, 10 psu) and (C) light irradiance (100 μmol m^{-2} s^{-1}, 30 μmol m^{-2} s^{-1}) (error bars = SD, $n = 2$). Known prymnesins were prymnesin-1: PRM-A (3Cl) + 2 pentose + hexose (green) and prymnesin-2: PRM-A (3Cl) + pentose (dark blue). (For interpretation of the references to colour in this figure legend, the reader is referred to the web version of this article.)

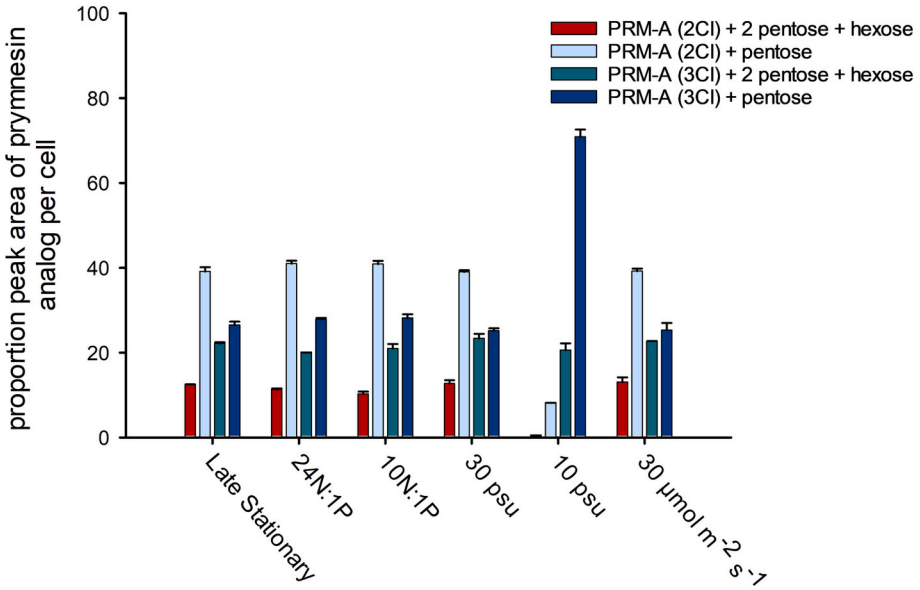

Fig. 5. Relative proportions of A-type prymnesin analogs in *P. parvum* UTEX-2797 harvested after growing for 30 d (late stationary phase) under different conditions (error bars = SD, $n = 2$). Known prymnesins were prymnesin-1: PRM-A (3Cl) + 2 pentose + hexose (dark green) and prymnesin-2: PRM-A (3Cl) + pentose (dark blue). (For interpretation of the references to colour in this figure legend, the reader is referred to the web version of this article.)

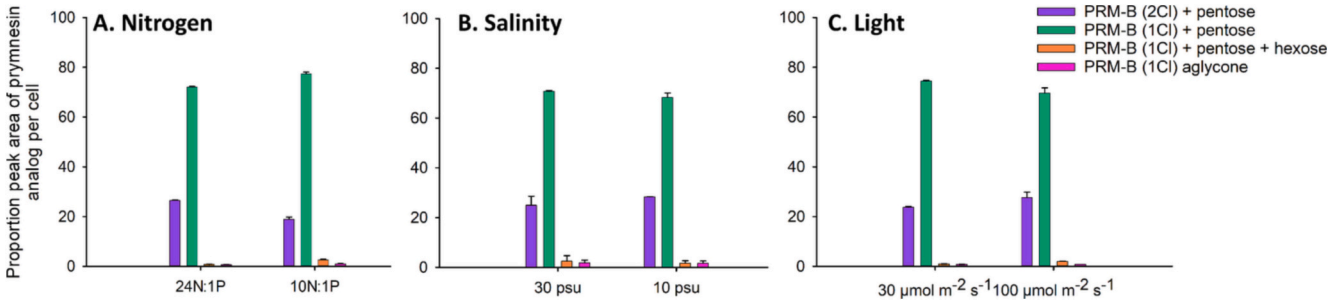

Fig. 6. Relative proportions of dominant B-type prymnesin analogs in *P. parvum* K-0374 harvested at day 10 grown in different conditions: (A) nitrogen availability (24N:1P, 10N:1P) (B) salinity (30 psu, 10 psu) and (C) light irradiance (30 µmol m^{-2} s^{-1}, 100 µmol m^{-2} s^{-1}) (error bars = SD, $n = 2$). Known prymnesin was prymnesin-B2: PRM-B (1Cl) + pentose (teal). (For interpretation of the references to colour in this figure legend, the reader is referred to the web version of this article.)

treatments at approximately ~72 %. (Fig. 9, Fig. S10). *P. parvum* PPSR01 prymnesin cell quotas showed similar trends to the other strains, where higher toxin levels were observed in late stationary phase in the 24N:1P medium compared to the 10N:1P medium and at a salinity of 30 psu compared to 10 psu (Fig. S11).

4. Discussion

Strain-specific toxicity has been demonstrated in various harmful algae like *Pseudo-nitzchia* and *Alexandrium* [25–27], and the same trend is believed to be true for *Prymnesium* [20]. In this study, strain-specific variability in prymnesin cell quotas and profiles across experimental conditions were observed. Prymnesin cell quotas at day 10 in *P. parvum* K-0374 were higher in cultures grown under lower light conditions, while in *P. parvum* UTEX-2797 and PPSR01 higher levels were observed under higher irradiance. A recent study gave similar results, with prymnesin cell quotas of two B-type producing strains, where *P. parvum* K-0374 responded similarly to this study with higher prymnesin cell quotas under low irradiance, while the other *P. parvum* strain had higher toxin levels with higher light irradiance [12]. In this work, the influence of abiotic and biotic factors had a more pronounced effect on the prymnesin profiles of *P. parvum* UTEX-2797 and PPSR01 than *P. parvum* K-0374. Specifically, the prymnesin profiles of *P. parvum* K-0374 remained similar across most treatments. Taken together, these findings suggest that factors influencing prymnesin profiles and quotas are strain-specific, and independent of growth rate.

Although strain-specific responses to different treatments were observed, there were some general trends shared across strains. Prymnesins were produced throughout the growth phases. However, the prymnesin profiles changed as cultures reached stationary phase. There is evidence that hemolytic activity of *P. parvum* cultures is highest in the stationary phase [13,14,28]. Increased toxicity during stationary phase could be associated with increased prymnesin concentration and/or with an increased proportion of specific prymnesin analogs. Within this study, an increased degree of glycosylation occurred in late stationary phase for all treatments. Increased glycosylation could be a result of carbohydrate accumulation in stationary phase as a means to dissipate photosynthetic energy [29], however this requires additional investigation. Two of the three strains studied exhibited a decreased degree of chlorination of prymnesins in stationary phase. After 30 days of growth, the prymnesin profiles of *P. parvum* UTEX-2797 had a higher proportion of prymnesin analogs with three chlorines relative to those containing two chlorines than at day 10 (Fig. S5). At the same time, *P. parvum* K-0374 shifted from di-chlorinated backbones to ones that contained only one chlorine (Fig. S7). However, this trend was not observed in *P. parvum* PPSR01, where the percentage of tri-chlorinated analogs in

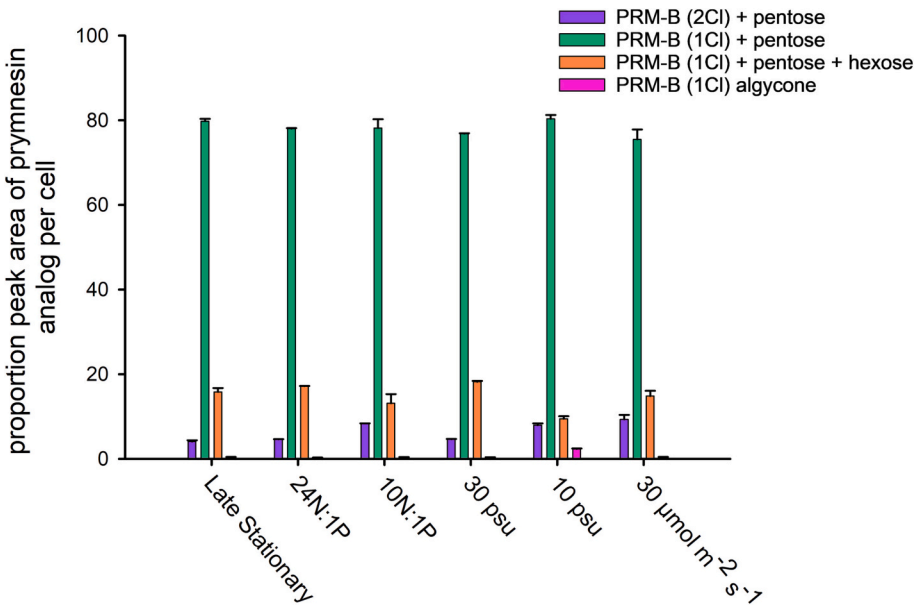

Fig. 7. Relative proportions of B-type prymnesin analogs in *P. parvum* K-0374 harvested after growing for 30 d (late stationary phase) under different conditions (error bars = SD, $n = 2$). Known prymnesin was prymnesin-B2: PRM-B (1Cl) + pentose (green). (For interpretation of the references to colour in this figure legend, the reader is referred to the web version of this article.)

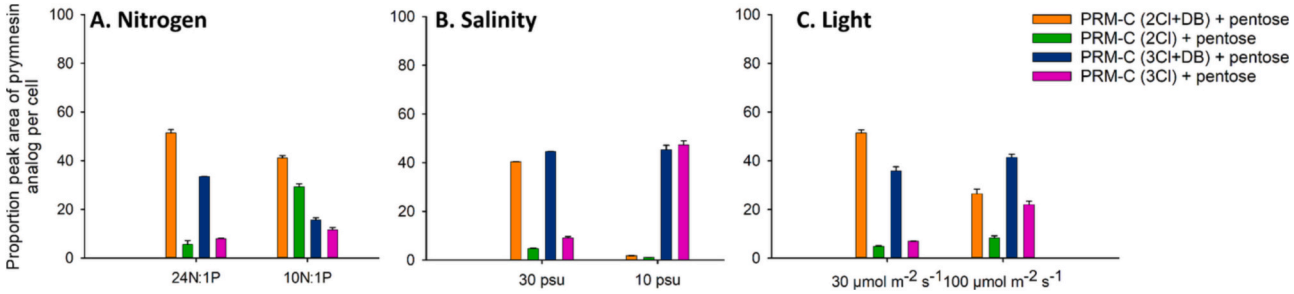

Fig. 8. Relative proportions of the four dominant C-type prymnesin (pentose) analogs in *P. parvum* PPSR01 harvested at day 10 grown in different conditions: (A) nitrogen availability (24N:1P, 10N:1P), (B) salinity (30 psu, 10 psu) and (C) light irradiance (30 µmol m^{-2} s^{-1}, 100 µmol m^{-2} s^{-1}) (error bars = SD, $n = 2$).

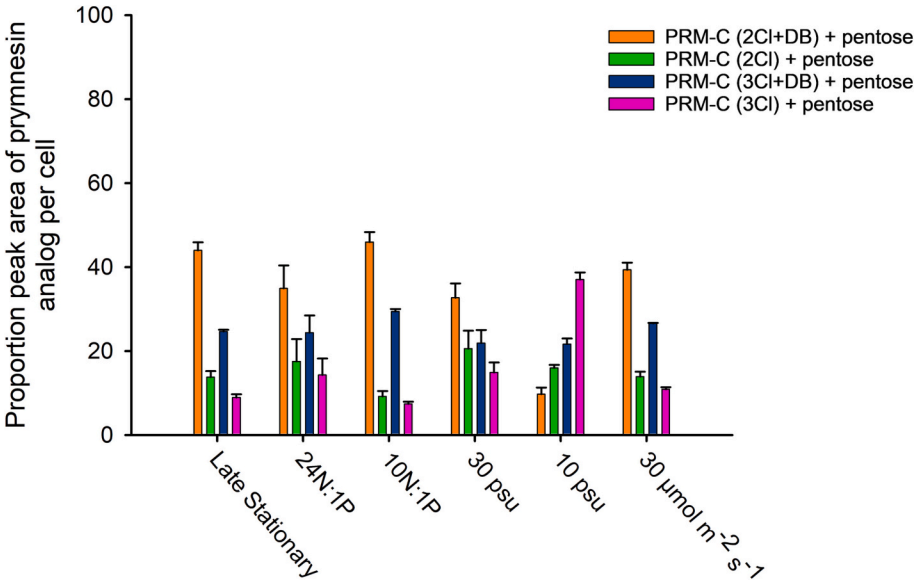

Fig. 9. Proportion of the for dominant C-type prymnesin (pentose) analogs per cell of *P. parvum* PPSR01 harvested after growing for 30 d (late stationary phase) under different conditions (error bars = SD, n = 2).

PPSR01 decreased from exponential phase into early stationary phase but increased again in late stationary phase (Fig. S8).

The effect that chlorination or glycosylation has on prymnesin toxicity has yet to be investigated due to the limited availability of isolated and structurally characterized prymnesin analogs. To date, the only comparison of relative toxicity has shown that the A-type triglycosylated prymnesin-1 and the singly glycosylated prymnesin-2 have similar ichthyotoxicity and hemolytic activity [30]. Prymnesin-2 and prymnesin-B1 had significantly different toxicities in the fish gill cell bioassay, with prymnesin-2 being six times more potent [9]. Both of these prymnesins are singly glycosylated, although they vary in their chlorination and backbone structures. In order to assess the effects of these structural variations, future work will need to focus on isolating and accurately quantifying individual prymnesin analogs with various levels of glycosylation, chlorination, and backbone structures to gain insights into analog-specific toxicity. This work has provided evidence of changes in abiotic factors and growth phases that control the production of these analogs, which can be exploited to target specific prymnesins for isolation, toxicity studies and reference material development.

Tri-chlorinated analogs dominated the profiles of *P. parvum* UTEX-2797 and PPSR01 when grown under low salinity with <5 % of the prymnesins being di-chlorinated when harvested after 10 days. While slightly higher levels of di-chlorination were observed in late stationary phase, the tri-chlorinated prymnesin analogs remained dominant. The cultures grown in 30 psu and 10 psu salinities were inoculated from cultures acclimated at 10 psu, however the cultures collected from 30 psu salinity showed similar profiles to the other treatments. This may imply a tightly controlled regulation of prymnesin production based on salinity conditions, the mechanisms of which warrant further investigation.

P. parvum cells tolerate a wide range of salinities, where optimal growth conditions may not align with toxicity [31,32]. The major changes observed in prymnesin profiles at lower salinity (10 psu) may be particularly relevant, as *P. parvum* blooms typically occur in lower salinities such as those in brackish waters (~3–8 psu) [31]. To date, there are no data for the prymnesin profiles during *P. parvum* blooms, but several studies have evaluated *P. parvum* toxicity at different salinities. Earlier studies showed that increased salinity results in lower toxicity of some *P. parvum* strains [33]. However, there have since been contradictory findings that suggest that salinity's influence on toxicity is strain-specific [7,18]. This agrees with results presented here, where changes were observed for *P. parvum* UTEX-2797 and PPSR01 strains, however, chlorination levels in *P. parvum* K-0374 were stable between the salinity treatments. It should be noted that the prymnesins in *P. parvum* K-0374 had lower degrees of chlorination. Taken together, these results from lower salinity media suggest that monitoring prymnesin profiles during harmful algal blooms may provide insight into the effects of changing environmental conditions on chlorination and toxicity of *P. parvum*.

This study focused on intracellular prymnesins, but due to recent studies showing that up to 30 % of prymnesins may be released into the media [12], we analyzed the media from each strain and treatment for the presence of prymnesins. The levels of prymnesins in the media (< 6 %) were lower in this study, appearing to be strain-specific and potentially influenced by both growth stage and abiotic factors. *P. parvum* PPSR01 consistently released <0.3 % of total prymnesins, while up to 6 % was released by *P. parvum* K-0374 (Fig. S3). The prymnesin profiles in the medium were not investigated further due to the low levels relative to the cells. The presence of different ratios of bacteria in the growth media (and possible photodegradation) may impact the extent of extracellular prymnesin profiles observed [12,34]. Cultures used in this study were not axenic, leading to the potential of bacterial lysis of algal cells and transformation of released prymnesins that could bias results obtained from the media [35]. In the future, comparing the profiles of intracellular and extracellular prymnesin analogs may provide additional information on the effects that biotransformation or photodegradation may have on the relative toxicity of prymnesins released into the environment.

Research on *P. parvum* toxicity to date has been limited by a lack of available reference materials. This study provides novel insight into the trends of prymnesin analogs associated with factors previously linked to differences in culture toxicity in some strains. Future work will focus on developing qualitative and quantitative reference materials, linking bioassays with prymnesin profiles, to further increase the understanding of prymnesin toxins, inform policy and support environmental monitoring of these algal biotoxins.

CRediT authorship contribution statement

Catherine C. Bannon: Conceptualization, Formal analysis, Investigation, Methodology, Visualization, Writing – original draft, Writing – review & editing. **Xinhui Wang:** Methodology, Resources. **Silvio Uhlig:** Funding acquisition, Writing – review & editing. **Ingunn A. Samdal:** Funding acquisition, Project administration, Writing – review & editing. **Pearse McCarron:** Conceptualization, Resources, Supervision, Writing – review & editing. **Thomas Ostenfeld Larsen:** Resources, Writing – review & editing. **Elizabeth M. Mudge:** Conceptualization, Supervision, Writing – original draft, Writing – review & editing.

Declaration of competing interest

The authors declare no conflict of interest.

Data availability

Data will be made available on request.

Acknowledgements

This study was carried out under the ToxANoWa project funded through the Research Council of Norway (Project No.: 314861). The authors would like to thank Nancy Lewis and Cheryl Rafuse for their training and assistance in the culturing facilities and internal reviews by Christopher O. Miles and Cheryl Rafuse of the manuscript prior to submission.

Appendix A. Supplementary data

Supplementary data to this article can be found online at https://doi.org/10.1016/j.algal.2024.103390.

References

[1] A. Larsen, W. Eikrem, E. Paasche, Growth and toxicity in *Prymnesium patelliferum* (Prymnesiophyceae) isolated from Norwegian waters, Can. J. Bot. 71 (1993) 1357–1362.
[2] D.L. Roelke, J.P. Grover, B.W. Brooks, J. Glass, D. Buzan, G.M. Southard, L. Fries, G.M. Gable, L. Schwierzke-Wade, M. Byrd, J. Nelson, A decade of fish-killing *Prymnesium parvum* blooms in Texas: roles of inflow and salinity, J. Plankton Res. 33 (2011) 243–253.
[3] G.M. Southard, L.T. Fries, A. Barkoh, *Prymnesium parvum:* the Texas experience, J. Am. Water Resour. Assoc. 46 (2010) 14–23.
[4] G. Free, W. Van de Bund, B. Gawlik, L. Van Wijk, M. Wood, E. Guagnini, K. Koutelos, A. Annunziato, B. Grizzetti, O. Vigiak, M. Gnecchi, S. Poikane, T. Christiansen, C. Whalley, F. Antognazza, B. Zerger, R.-J. Hoeve, H. Stielstra, An EU Analysis of the Ecological Disaster in the Oder River of 2022, EUR 31418 EN, Publications Office of the European Union, Luxembourg, 2023, pp. JRC132271.
[5] J. Sobieraj, D. Metelski, Insights into toxic *Prymnesium parvum* blooms as a cause of the ecological disaster on the Odra River, Toxins 15 (2023) 403.
[6] S.R. Manning, J.W. La Claire, Isolation of polyketides from *Prymnesium parvum* (Haptophyta) and their detection by liquid chromatography/mass spectrometry metabolic fingerprint analysis, Anal. Biochem. 442 (2013) 189–195.
[7] E. Granéli, P.S. Salomon, Factors influencing allelopathy and toxicity in *Prymnesium parvum*, J. Am. Water Resour. Assoc. 46 (2010) 108–120.
[8] T. Igarashi, M. Satake, T. Yasumoto, Structures and partial stereochemical assignments for prymnesin-1 and prymnesin-2: potent hemolytic and ichthyotoxic glycosides isolated from the red tide alga *Prymnesium parvum*, J. Am. Chem. Soc. 121 (1999) 8499–8511.

[9] S.A. Rasmussen, S. Meier, N.G. Andersen, H.E. Blossom, J.Ø. Duus, K.F. Nielsen, P. J. Hansen, T.O. Larsen, Chemodiversity of ladder-frame prymnesin polyethers in *Prymnesium parvum*, J. Nat. Prod. 79 (2016) 2250–2256.
[10] T. Igarashi, M. Satake, T. Yasumoto, Prymnesin-2: a potent ichthyotoxic and hemolytic glycoside isolated from the red tide alga *Prymnesium parvum*, J. Am. Chem. Soc. 118 (1996) 479–480.
[11] S.B. Binzer, D.K. Svenssen, N. Daugbjerg, C. Alves-de-Souza, E. Pinto, P.J. Hansen, T.O. Larsen, E. Varga, A-, B- and C-type prymnesins are clade specific compounds and chemotaxonomic markers in *Prymnesium parvum*, Harmful Algae 81 (2019) 10–17.
[12] N. Medić, E. Varga, D.B. Van de Waal, T.O. Larsen, P.J. Hansen, The coupling between irradiance, growth, photosynthesis and prymnesin cell quota and production in two strains of the bloom-forming haptophyte, *Prymnesium parvum*, Harmful Algae 112 (2022) 102173.
[13] M. Shilo, Formation and mode of action of algal toxins, Bacteriol. Rev. 31 (1967) 180–193.
[14] N. Johansson, E. Granéli, Influence of different nutrient conditions on cell density, chemical composition and toxicity of *Prymnesium parvum* (Haptophyta) in semi-continuous cultures, J. Exp. Mar. Biol. Ecol. 239 (1999) 243–258.
[15] E. Granéli, N. Johansson, Increase in the production of allelopathic substances by *Prymnesium parvum* cells grown under N- or P-deficient conditions, Harmful Algae 2 (2003) 135–145.
[16] E. Granéli, B. Edvardsen, D.L. Roelke, J.A. Hagström, The ecophysiology and bloom dynamics of *Prymnesium* spp, Harmful Algae 14 (2012) 260–270.
[17] E. Lindehoff, E. Granéli, W. Granéli, Effect of tertiary sewage effluent additions on *Prymnesium parvum* cell toxicity and stable isotope ratios, Harmful Algae 8 (2009) 247–253.
[18] D.A. Caron, A.A.Y. Lie, T. Buckowski, J. Turner, K. Frabotta, The effect of pH and salinity on the toxicity and growth of the golden alga, *Prymnesium parvum*, Protist 174 (2023) 125927.
[19] K.D. Hambright, J.D. Easton, R.M. Zamor, J. Beyer, A.C. Easton, B. Allison, Regulation of growth and toxicity of a mixotrophic microbe: implications for understanding range expansion in *Prymnesium parvum*, Freshwater Sci. 33 (2014) 745–754.
[20] A. Larsen, S. Bryant, U. Båmstedt, Growth rate and toxicity of *Prymnesium parvum* and *Prymnesium patelliferum* (Haptophyta) in response to changes in salinity, light and temperature, Sarsia 83 (1998) 409–418.
[21] B.N. Hill, G.N. Saari, W.B. Steele, J. Corrales, B.W. Brooks, Nutrients and salinity influence *Prymnesium parvum* (UTEX LB 2797) elicited sublethal toxicity in *Pimephales promelas* and *Danio rerio*, Harmful Algae 93 (2020) 101795.
[22] D.K. Svenssen, S.B. Binzer, N. Medić, P.J. Hansen, T.O. Larsen, E. Varga, Development of an indirect quantitation method to assess ichthyotoxic B-type prymnesins from *Prymnesium parvum*, Toxins 11 (2019) 251.
[23] R.R.L. Guillard, P.E. Hargraves, *Stichochrysis immobilis* is a diatom, not a chrysophyte, Phycologia 32 (1993) 234–236.
[24] V.M. Lundgren, P.M. Glibert, E. Granéli, N.K. Vidyarathna, E. Fiori, L. Ou, K. J. Flynn, A. Mitra, D.K. Stoecker, P.J. Hansen, Metabolic and physiological changes in Prymnesium parvum when grown under, and grazing on prey of, variable nitrogen:phosphorus stoichiometry, Harmful Algae 55 (2016) 1–12.
[25] C.A. Scholin, M.C. Villac, K.R. Buck, J.M. Krupp, D.A. Powers, G.A. Fryxell, F. P. Chavez, Ribosomal DNA sequences discriminate among toxic and non-toxic *Pseudonitzschia* species, Nat. Toxins 2 (1994) 152–165.
[26] A.E. Thessen, H.A. Bowers, D.K. Stoecker, Intra- and interspecies differences in growth and toxicity of *Pseudo-nitzschia* while using different nitrogen sources, Harmful Algae 8 (2009) 792–810.
[27] K. Ichimi, T. Suzuki, A. Ito, Variety of PSP toxin profiles in various culture strains of *Alexandrium tamarense* and change of toxin profile in natural *A. tamarense* population, J. Exp. Mar. Biol. Ecol. 273 (2002) 51–60.
[28] J. Qin, Z. Hu, Q. Zhang, N. Xu, Y. Yang, Toxic effects and mechanisms of *Prymnesium parvum* (Haptophyta) isolated from the Pearl River estuary, China, Harmful Algae 96 (2020) 101844.
[29] K.H. Halsey, B.M. Jones, Phytoplankton strategies for photosynthetic energy allocation, Annu. Rev. Mar. Science 7 (2015) 265–297.
[30] T. Igarashi, S. Aritake, T. Yasumoto, Biological activities of prymnesin-2 isolated from a red tide alga *Prymnesium parvum*, Nat. Toxins 6 (1998) 35–41.
[31] S.R. Manning, J.W. La Claire, Prymnesins: toxic metabolites of the golden alga, *Prymnesium parvum* Carter (Haptophyta), Mar. Drugs 8 (2010) 678–704.
[32] D.L. Roelke, A. Barkoh, B.W. Brooks, J.P. Grover, K.D. Hambright, J.W. LaClaire, P. D.R. Moeller, R. Patino, A chronicle of a killer alga in the west: ecology, assessment, and management of *Prymnesium parvum* blooms, Hydrobiologia 764 (2016) 29–50.
[33] G.M. Padilla, Growth and toxigenesis of the chrysomonad *Prymnesium parvum* as a function of salinity, J. Protozool. 17 (1970) 456–462.
[34] R.B. Taylor, B.N. Hill, L.M. Langan, C.K. Chambliss, B.W. Brooks, Sunlight concurrently reduces *Prymnesium parvum* elicited acute toxicity to fish and prymnesins, Chemosphere 263 (2021) 127927.
[35] M. Wang, S. Chen, W. Zhou, W. Yuan, D. Wang, Algal cell lysis by bacteria: a review and comparison to conventional methods, Algal Res. 46 (2020) 101794.